Topographic Analysis of the Choriocapillaris in Intermediate Age-related Macular Degeneration

ENRICO BORRELLI, YUE SHI, AKIHITO UJI, SIVA BALASUBRAMANIAN, MARCO NASSISI, DAVID SARRAF, AND SRINIVAS R. SADDA

- PURPOSE: To quantitate regional differences in the choriocapillaris (CC) of patients with intermediate age-related macular degeneration (iAMD), using swept-source optical coherence tomography angiography (SS-OCTA) imaging.
- DESIGN: Cross-sectional study.
- METHODS: Subjects were imaged with the SS-OCTA system (PLEX Elite 9000, Carl Zeiss Meditec Inc, Dublin, California, USA). The CC en face images were first compensated for the signal attenuation caused by drusen by using the structural information from the same slab. Subsequently, for each eye, 2 compensated CC en face images generated from 2 different OCTA volume scan sets were registered and averaged. The averaged CC images were then exported to ImageJ and binarized for subsequent quantitative analysis. In addition to the analysis of the whole averaged CC en face image in iAMD eyes, quantitative analysis was also performed in 3 different regions: (1) drusen region, (2) 150-μm-wide ring around the drusen border, and (3) drusen-free region.
- RESULTS: Thirty eyes (30 patients) with iAMD and 30 healthy eyes from 30 controls were enrolled. Compared with controls, iAMD eyes displayed a lower number of signal voids (median and interquartile range [IQR]: 2561 and 2343-2746 vs 2734 and 2558-2834; $P = .013$), a greater signal void average size (median, IQR: 581.9 μm^2, 466.1-726.9 μm^2 vs 503.8 μm^2, 429.1-576.8 μm^2; $P = .027$), and a greater total signal void area (median, IQR: 26.0%, 22.1%-29.6% vs 23.8%, 21.2%-26.4%; $P = .038$). In multiple regression analysis, the presence of iAMD was not significantly associated with any of the CC variables. By contrast, the drusen region area was significantly associated with CC alterations. In the evaluation of the iAMD group, both the area underneath drusen and the 150-μm-wide ring region around drusen were characterized by an increased total signal void area ($P = .005$ and $P = .045$, respectively) vs the drusen-free region.
- CONCLUSIONS: Intermediate AMD eyes demonstrated increased CC flow impairment, which co-localizes to the area of CC beneath and immediately surrounding drusen. (Am J Ophthalmol 2018;196:34–43. © 2018 Elsevier Inc. All rights reserved.)

THE CHORIOCAPILLARIS (CC) CONSTITUTES THE innermost portion of the choroidal vasculature and is composed of a dense meshwork of freely anastomosing capillaries that serve as the main source of nutrition and oxygenation for the retinal pigment epithelium (RPE) and the outer retinal layers. Histopathologic abnormalities of the CC have been extensively investigated in age-related macular degeneration (AMD).[1–3] Although several factors are thought to be implicated in the pathogenesis of this disorder, a strong body of evidence suggests that the development and progression of AMD may be driven by choroidal ischemia causing disruption of the RPE-Bruch complex and loss of the photoreceptors.[4–6]

Optical coherence tomography angiography (OCTA) has significantly advanced our power to visualize and quantify the retinal and choroidal microvasculature with depth-resolved capability. Recently, en face OCTA analysis at the level of the CC has illustrated small dark regions, or flow voids, that alternate with granular bright areas of CC flow and that may represent CC nonperfusion.[7] CC flow voids have recently been renamed signal voids, because the small dark regions may alternatively represent a flow signal strength below the decorrelation threshold that will be undetectable in the en face image.[8,9]

Several studies have investigated the CC in early and intermediate AMD using OCTA. The main limitation of these prior studies, however, relates to the spectral-domain nature of the OCTA system that was used. Typically a wavelength around 840 nm is employed that may be attenuated by the presence of drusen, leading to shadowing artifacts that may confound the analysis.[10] Swept-source (SS) OCTA systems, however, provide greater sensitivity and a longer wavelength that improves RPE penetration and decreases shadowing artifacts, and improve the ability to study the CC in AMD eyes (Figure 1).
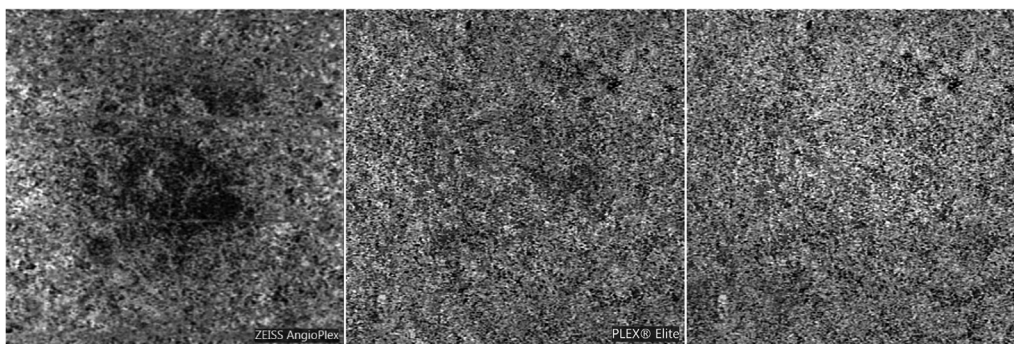
FIGURE 1. Example of false optical coherence tomography angiography (OCTA) signal loss on the spectral-domain (SD) system. En face SD-OCTA choriocapillaris slab (Left) shows several areas of signal loss underlying drusen. Note that there is no signal loss on the en face SS-OCTA image (Middle) within the corresponding regions. Given the presence of this discordance between these 2 images, we may conclude that there is a false signal loss in the SD-OCTA image. The en face SS-OCTA image was further improved by compensating with choriocapillaris structure information (Right).

Previous histopathologic studies have suggested that the formation of drusen may not be spatially random but may be influenced by the anatomy of the underlying choriocapillaris.[2,11,12] Therefore, we hypothesized that the CC with OCTA may illustrate zonal differences with and without drusen. Therefore, the main aim of this study was to explore regional quantitative differences in the CC of patients affected by intermediate AMD (iAMD), using SS-OCTA analysis that may provide more reliable data than similar studies previously completed using spectral-domain OCTA (SD-OCTA).

METHODS

• STUDY PARTICIPANTS: This study was a prospective, observational, case-control analysis. Patients 50 years of age with a clinical diagnosis of intermediate AMD in at least 1 eye were enrolled from the medical retina clinics affiliated with the Doheny-UCLA Eye Center. The study was approved by the UCLA Institutional Review Board and adhered to the tenets of the Declaration of Helsinki and the Health Insurance Portability and Accountability Act. Written informed consent was obtained from all subjects prior to enrollment in the study.

All patients were consecutively enrolled between May and October 2017 and received a complete ophthalmologic examination, which included the measurement of best-corrected visual acuity (BCVA), intraocular pressure (IOP), and dilated ophthalmoscopy. BCVA measurements were made using a Snellen chart and were converted to the logarithm of the minimum angle of resolution (logMAR), as previously described.[13]

The inclusion criteria for iAMD eyes included drusen > 125 μm in diameter with or without pigmentary abnormalities as determined by the retinal physician during clinical examination and confirmed by dense-volume OCT (pigment abnormalities on OCT manifesting as intraretinal hyperreflective foci). Exclusion criteria for iAMD eyes were as follows: (1) previous ocular surgery or history of anti–vascular endothelial growth factor (VEGF) therapy; (2) myopia greater than -3.00 diopters; (3) presence of reticular pseudodrusen with OCT analysis, since its presence was demonstrated to be associated with a reduced CC flow[14]; (4) any maculopathy secondary to causes other than AMD (including presence of vitreomacular traction syndrome or an epiretinal mebrane); and (5) presence of pigment epithelium detachment causing shadowing artifact, defined as a hyporeflective OCT signal in the corresponding area as identified on the en face OCT CC slab and associated OCT B-scans (as assessed by 2 Doheny Imaging Reading Center certified graders: E.B. and S.B.).

Because age may influence quantitative measurements of the retinal and choroidal vasculature on OCTA,[15,16] a control group similar with respect to age and sex was also included in the current analysis. All control subjects failed to demonstrate evidence of ocular disease or media opacity as evaluated by dilated fundus examination, OCT, and OCTA analysis.

• IMAGING: Patients underwent SS-OCTA imaging using the PLEX Elite 9000 device (Carl Zeiss Meditec Inc, Dublin, California, USA), which uses a swept laser source with a central wavelength of 1050 nm (1000-1100 nm full bandwidth) and operates at 100 000 A-scans per second. This instrument employs a full-width at half-maximum (FWHM)[13] axial resolution of approximately 5 μm in tissue, and a lateral resolution at the retinal surface estimated at approximately 14 μm. OCTA imaging of the macula included a 3 × 3-mm area centered on the fovea (300 A-scans × 300 B-scans). One eye per individual was randomly selected (in patients with

bilateral intermediate AMD and in healthy controls) and repeatedly imaged with pupil dilation to obtain 2 OCTA volume scan sets with sufficient image quality (signal strength index > 7) that fulfilled the acceptance criteria of the Doheny Image Reading Center, as previously reported.[17,18]

A fully automated retinal layer segmentation algorithm was applied to the 3-dimensional structural OCT data, in order to segment the CC slab as defined previously (10 μm thick starting 31 μm posterior to the RPE fit reference, which corresponds to the inner border of the RPE in absence of drusen).[16] The RPE fit reference was manually adjusted in those cases in which the fully automated algorithm failed to select the correct segmentation. This segmentation was then applied to OCTA flow intensity and structural data to obtain vascular and structural images of the choriocapillaris, respectively.

• IMAGE PROCESSING: *Compensation for the Signal Attenuation Under Drusen.* To eliminate the influence of the shadowing effect on the quantitation of the CC, we used the structural signal from the choriocapillaris, as previously shown.[19] In brief, we first exported the en face image of the CC obtained with maximum projection analyses and the correspondent en face CC structural image. The 2 images were then imported in ImageJ software, version 1.50 (National Institutes of Health, Bethesda, Maryland, USA; available at http://rsb.info.nih.gov/ij/index.html),[20] and an inverse transformation and a Gaussian smoothing filter were applied to the structural image. After this transformation, a multiplication between the en face CC flow image and the smoothed, inverted CC structural image was performed, as follows:

$$F_{compensated} = F_{cc} * (1 - Norm(S_{cc})) \qquad (1)$$

where Norm() represents the normalization operation of the image, S_{CC} is the structural CC image, and F_{CC} is the CC flow image. Finally, the compensated choriocapillaris flow image was obtained (Figure 1).

Image Registration and Averaging. Two CC en face images generated from 2 different OCTA cube scan sets were stacked to create a 2-frame video and were registered before multiple image averaging. A central square area of 819 × 819 pixels was cropped for registration and averaging. Registration was first performed on the 2-frame video based on the superficial capillary plexus en face images, as previously shown.[17] This same transformation was then applied to the CC layer, as described in detail in a previous publication.[21] After registration, the 2 frames of the choriocapillaris were compounded into a single image by projecting the average intensity (Figure 2). The first of the 2 images used to obtain the averaged CC image was used in the analysis comparing single and averaged CC images.

Quantitative Image Analysis. The obtained averaged CC en face image was then binarized for quantitative image analysis of the signal voids. The Phansalkar method (radius, 15 pixels) was used to binarize the images, as previously described.[9,16,21] These images were then processed with the "Analyze Particles" command, in order to count and measure the flow voids. The average size of the signal voids was calculated in μm^2, using the conversion formula [area in μm^2 = (average size in pixels) × (3 × 10^6/1024)^2], since the exported image has a resolution of 1024 × 1024 and covers a 3 × 3-mm macular cube area.

The CC directly beneath major superficial retinal vessels was excluded from analysis to eliminate potentially confounding shadow or projection artifacts, as previously described.[18,22]

In iAMD eyes, the quantitative analysis was performed over the whole averaged CC en face image, in addition to 3 different regions: (1) *drusen region*, in order to investigate the CC directly beneath drusen, (2) *150-μm-wide ring around the drusen edge* to assess the CC neighboring drusen, and (3) *drusen-free region* (Figure 2).

To obtain the drusen region, we created a map of the drusen using an en face structural OCT slab (∼28 μm thick) at the level of the RPE, as previously described.[14] This slab, which highlights drusen elevating the RPE as hyporeflective lesions, was enhanced with the "brightness/contrast improvement" ImageJ function to increase the contrast between drusen and the surrounding non-drusen area, and then binarized (Figure 2).

To obtain the 150-μm-wide ring around the drusen edge, we used the "Distance Map" ImageJ function on the "drusen region" image that was already generated and binarized. This function provided delineation of a border 150 μm displaced from the drusen edge (Figures 2-4). Furthermore, the "Distance Map" function on the "binarized" image allowed us to delimit those areas within 150 μm of the edge of all the drusen in the image (without any size limit), by excluding areas occupied by adjacent drusen (Figure 4). The remaining region was termed the "drusen-free region" (Figures 2-4). Of note, in the regional evaluation of the CC we did not investigate differences in the average flow void size, since the presence of signal voids extending across 2 contiguous regions could potentially confound the analysis.

• STATISTICAL ANALYSIS: All quantitative variables were reported as mean and standard deviation (SD) or median and interquartile range (IQR) in the Results section and in the tables.

To detect departures from normality distribution, Shapiro-Wilk test was performed for all variables. Student *t* test and nonparametric Mann-Whitney *U* test were conducted to investigate differences in continuous variables between the AMD and control groups. The relationship between each CC variable (considered as dependent
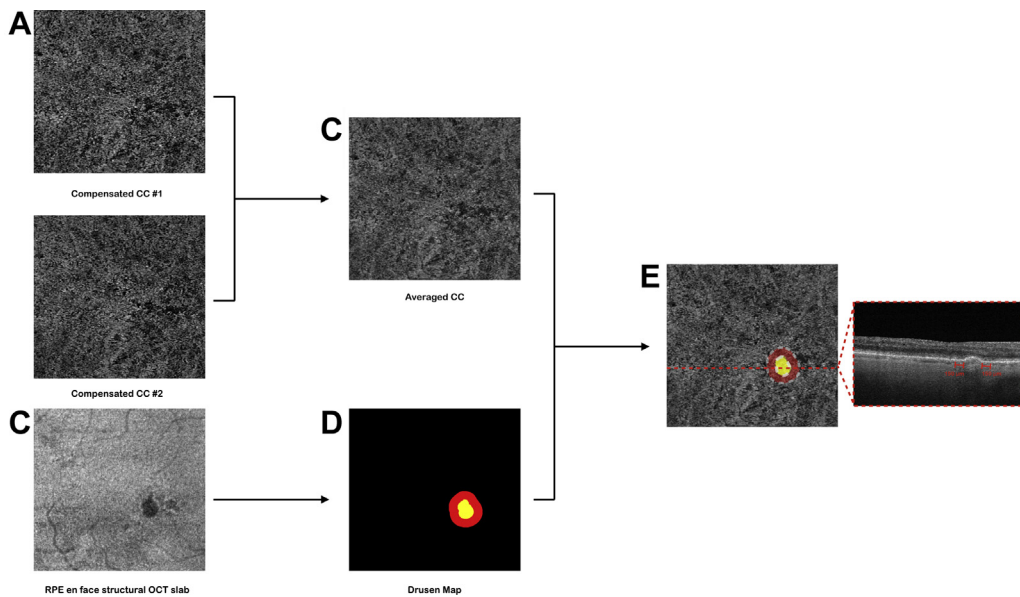
FIGURE 2. Representation of the algorithm used to investigate the choriocapillaris (CC). Two CC en face images compensated with CC structure information (a: CC #1 and CC #2) generated from 2 OCTA cube scan sets were registered and averaged (b: Averaged CC). In intermediate age-related macular degeneration (AMD) eyes, in addition to the analysis of the whole averaged CC en face image, we performed a regional analysis related to the presence of overlying drusen. We created a drusen map (d) using the en face structural OCT slab (c: ∼28 μm thick) segmented at the level of the retinal pigment epithelium (RPE). In the final image (e), the assessment of the CC was thus performed in 3 different regions: (1) "drusen region" (yellow in the final image), in order to investigate the CC region directly beneath drusen, (2) "150-μm-wide ring around the drusen edge" region (red) to assess the CC near drusen, and (3) "drusen-free" region, which was the remaining black area.
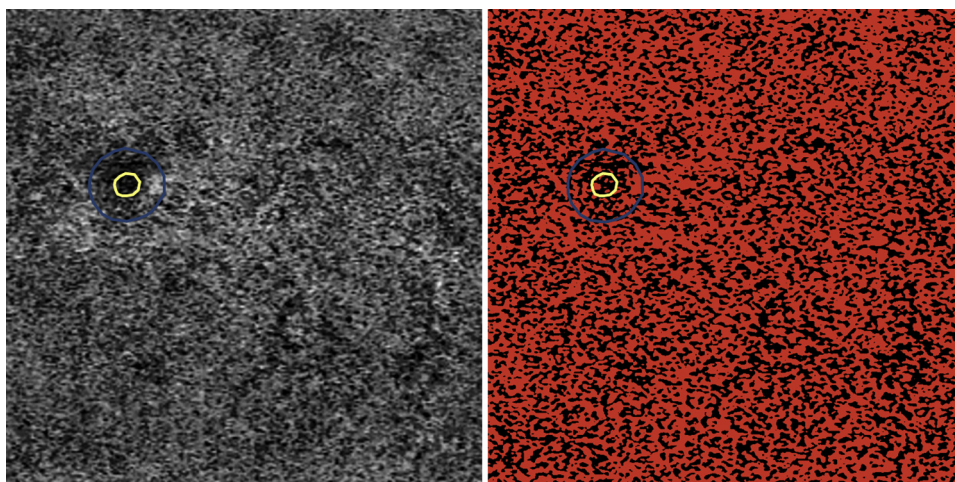

FIGURE 3. Representative choriocapillaris images from an intermediate age-related macular degeneration eye with a single druse. The compensated and averaged choriocapillaris image (Left) was binarized (Right) in order to investigate several quantitative variables. This assessment was performed in 3 different regions: (1) "drusen region" (circumscribed in yellow in the images), (2) "150-μm-wide ring around the drusen" region (circumscribed in blue), and (3) "drusen-free" region (the remaining region).

variables) and other parameters was investigated with a multiple linear regression analysis. Q-Q plots of regression standardized residuals were constructed to confirm that the residuals were characterized by a normal distribution. Nonparametric Friedman test was conducted to investigate regional differences in quantitative CC variables within the AMD group. Related-samples Wilcoxon signed rank test was conducted to compare single and averaged CC
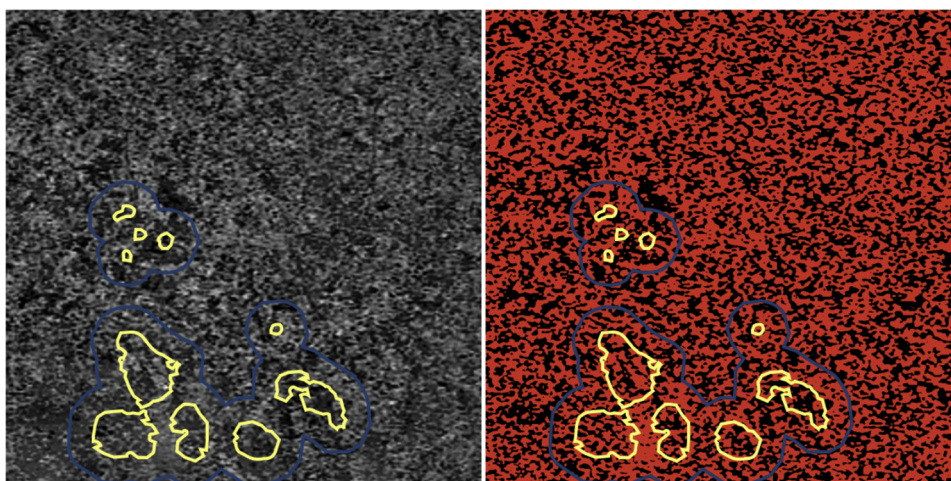
FIGURE 4. Representative choriocapillaris images from an eye with intermediate age-related macular degeneration and confluent drusen. Compensated and averaged choriocapillaris image (Left), which was binarized (Right) to investigate several quantitative variables. In these cases with confluent drusen, the processed images included the area directly beneath drusen (delimited in yellow in the images) in the "drusen region." In the "150-μm-wide ring around the drusen" region, those areas within 150 μm from the edge of all the drusen in the image (circumscribed in blue) were included, by excluding areas occupied by adjacent drusen.

images. Statistical calculations were performed using Statistical Package for Social Sciences (version 20.0, SPSS Inc, Chicago, Illinois, USA). The chosen level of statistical significance was $P < .05$.

RESULTS

• CHARACTERISTICS OF PATIENTS INCLUDED IN THE ANALYSIS: Of the 60 patients included in this analysis, 30 (21 female) were diagnosed with iAMD and 30 (22 female) were healthy controls. In the iAMD group, 21 patients presented with bilateral intermediate AMD, whereas 9 patients presented with neovascular AMD in the fellow eye.

Mean ± SD age was 78.7 ± 7.7 years (range 66-93 years) in the iAMD group and 74.2 ± 10.0 years (range 53-93 years) in the control group ($P = .055$). The overall demographic and clinical characteristics of the 2 groups are shown in Table 1.

• COMPARISON BETWEEN THE 2 GROUPS: The median number of signal voids was 2734 (IQR = 2558-2834) in the control group and 2561 (IQR = 2343-2746) in the iAMD group ($P = .013$). The average size of the signal voids was increased in iAMD eyes (median: 581.9 μm^2 and IQR: 466.1-726.9 μm^2 in the iAMD group; median: 503.8 μm^2 and IQR: 429.1-576.8 μm^2 in the normal group; $P = .027$). The total signal void area was significantly increased in iAMD eyes compared to control eyes (median: 26.0% and IQR 22.1%-29.6% in the iAMD group; median: 23.8% and IQR: 21.2%-26.4% in the normal group; $P = .038$) (Table 2).

• REGRESSION ANALYSIS: In multiple regression analysis (Table 3), the presence of intermediate AMD was not significantly associated with any of these CC variables. The size of the drusen region, however, was significantly associated with a reduced number of signal voids ($P = .033$), a greater total signal void area ($P = .018$) and average signal void size ($P = .023$). The latter analysis showed that CC alterations correlated with the extent of drusen and were observed independent of the AMD diagnosis.

A separate analysis comparing the entire CC area in control eyes and the drusen-free region in iAMD was also performed. In multiple regression analysis, only age was associated with the CC variables (Table 4). Even after performing a backward stepwise multiple regression analysis, only age was associated with the CC variables.

• REGIONAL EVALUATION OF THE CHORIOCAPILLARIS IN INTERMEDIATE AGE-RELATED MACULAR DEGENERATION EYES: In the iAMD group, both the drusen and the 150-μm-wide peri-drusen ring regions were characterized by an increased total signal void area ($P = .005$ and $P = .045$, respectively), compared to the drusen-free region. The total signal void area was slightly greater numerically in the drusen region than in the 150-μm-wide peri-drusen ring region, although this difference did not reach the statistical significance ($P = .071$) (Table 5).

• COMPARISON BETWEEN SINGLE AND AVERAGED IMAGES: Table 6 summarizes the comparisons between single and averaged CC images. In both the analysis considering the whole study cohort and that analyzing the individual subgroups, the averaged CC images showed

TABLE 1. Demographic and Clinical Characteristics of Controls and Age-related Macular Degeneration Patients

	Controls	Intermediate AMD	P Value
Number of patients (eyes)	30 (30)	30 (30)	-
Age (years), mean ± SD	74.2 ± 10.0	78.7 ± 7.7	.055[a]
Sex (n)			
Female	22	21	1.0[b]
Male	8	9	
BCVA (logMAR), median (IQR)	0.0 (0.0-0.1)	0.1 (0.0-0.2)	.005[c]
Diabetes (n)	5	4	1.0[b]
Drusen area (mm²), mean ± SD	0.00 ± 0.00	0.23 ± 0.16	<.0001

AMD = age-related macular degeneration; BCVA = best-corrected visual acuity; IQR = interquartile range; logMAR = logarithm of the minimum angle of resolution.
[a]By t test.
[b]By Fisher exact test.
[c]By Mann-Whitney U test.

TABLE 2. Tested Choriocapillaris Optical Coherence Tomography Variables in Controls and Age-related Macular Degeneration Patients

	Control	Intermediate AMD	P Value
No. of signal voids	2734 (2558–2834)	2561 (2343–2746)	.013
Total signal void area (%)	23.8 (21.2–26.4)	26.0 (22.1–29.6)	.038
Average size of the signal voids (μm²)	503.8 (429.1–576.8)	581.9 (466.1–726.9)	.027

AMD = age-related macular degeneration.
Data are presented as median (interquartile range).
Comparisons were performed using Mann-Whitney U test.

TABLE 3. Multiple Regression Analysis of Optical Coherence Tomography Angiography Variables

	No. of Signal Voids				Total Signal Void Area				Average Size of the Signal Voids			
	B	Standard Error	Standardized ß Coefficient	P Value	B	Standard Error	Standardized ß Coefficient	P Value	B	Standard Error	Standardized ß Coefficient	P Value
Age	-1.228	3.235	-0.244	.056	.108	.059	0.231	.124	.315	.190	0.305	.017
Intermediate AMD	78.561	67.005	0.065	.657	-.966	1.231	-0.035	.812	-2.934	3.928	-0.043	.764
Size of drusen region	-307.163	86.580	-0.323	.033	6.952	1.591	0.307	.018	33.972	5.706	0.295	.023

AMD = age-related macular degeneration.

significant differences compared to the single CC images. Specifically, the averaged images were characterized by (1) a reduction in number of signal voids, (2) an increase in total signal void area, and (3) a reduction in size of the signal voids.

DISCUSSION

IN THIS CROSS-SECTIONAL STUDY WE PROSPECTIVELY investigated CC features in intermediate AMD eyes with SS-OCTA. Overall, we observed that intermediate AMD

TABLE 4. Multiple Regression Analysis Between Optical Coherence Tomography Angiography Variables and Other Parameters, Considering Only the Drusen-Free Area in Age-related Macular Degeneration Eyes

	Total Signal Void Area				Average Size of the Signal Voids			
	B	Standard Error	Standardized ß Coefficient	P Value			Standardized ß Coefficient	P Value
Age	.109	.060	0.305	.020	.353	.168	0.301	.021
Intermediate AMD	-1.767	1.244	-0.210	.165	-7.413	3.479	-0.247	.103
Drusen area	.910	1.607	-0.030	.763	2.350	4.459	-0.109	.460

AMD = age-related macular degeneration.

TABLE 5. Regional Evaluation of the Choriocapillaris in Intermediate Age-related Macular Degeneration Eyes

	AMD		
	Drusen Area	150-μm Drusen Ring Area	Drusen-Free Area
Total signal void area (%)	28.5 (23.0–35.0)	26.5 (22.5–30.7)	24.8 (20.9–28.6)
		.071[a]	.005[a]
	-		.045[b]

AMD = age-related macular degeneration.
[a]Friedman test: comparison vs "Drusen Area."
[b]Friedman test: comparison cs "150-μm Drusen Ring Area."

TABLE 6. Tested Choriocapillaris Optical Coherence Tomography Variables in Single and Averaged Images

	Single CC Image	Averaged CC Image	P Value
Whole study cohort			
No. of signal voids	2143 (1836–2405)	2652 (2440–2824)	<.0001
Total signal void area (%)	33.5 (30.4–36.8)	25.0 (21.7–28.8)	<.0001
Average size of the signal voids (μm²)	912.4 (723.5–1157.0)	418.7 61.9 (356.1 52.0–537.1 80.9)	<.0001
Intermediate AMD group			
No. of signal voids	1944 (1750–2371)	2561 (2343–2746)	<.0001
Total signal void area (%)	34.7 (31.5–37.4)	26.0 (22.1–29.6)	<.0001
Average size of the signal voids (μm²)	1023.9 (763.9–1235.1)	581.9 (466.1–726.9)	<.0001
Control group			
No. of signal voids	2278 (1984–2494)	2734 (2558–2834)	<.0001
Total signal void area (%)	32.0 (28.9–35.8)	23.8 (21.2–26.4)	<.0001
Average size of the signal voids (μm²)	794.8 (659.2–1040.3)	503.8 (429.1–576.8)	<.0001

AMD = age-related macular degeneration; CC = choriocapillaris.
Data are presented as median (interquartile range).
Comparisons were performed using related-samples Wilcoxon signed rank test.

eyes are characterized by significant CC flow alterations that topographically co-localize with the presence of drusen. Of note, this study employed swept-source technology with image averaging analysis that may significantly improve the reliability of data acquisition.

Our group has recently described the importance of averaging multiple en face images to optimize evaluation of the CC with OCTA.[21] In this previous publication,[21] 17 eyes of 17 healthy patients were repeatedly scanned to obtain 9 CC en face images, which were registered and averaged. Not only did averaging improve CC visualization, but quantitative measures of the CC were also affected. For example, averaged images showed a reduction in the total signal void area, which was consistent with the observation

that the flow pattern in the CC changed between different frames, even after registration. Several theories were proposed to explain this finding: (1) averaging may improve the capability to distinguish real vs false signal voids, since the vascular flow pattern may be influenced by the decorrelation signal, which may vary from scan to scan; (2) minor differences in segmentation may affect the CC en face image analysis; and (3) true dynamic flow changes may occur from frame to frame. In the present study, we registered and averaged only 2 CC scans for each patient; however, we consistently recognized changes in the flow pattern from frame to frame that resulted in a reduced total signal void area after averaging, in both AMD and healthy eyes.

Data from a number of studies using distinct approaches indicate that microvascular choroidal changes are associated with early and intermediate AMD. Histopathologic studies have demonstrated that CC alterations increase with age and the presence of drusen.[1–3] Interestingly, the formation of drusen may not be spatially random but may be influenced by the anatomy of the underlying CC.[11,12] Mullins and associates[2] have extensively studied the causative relationship between outer retinal layer alterations and CC impairment. They analyzed postmortem eyes from 45 subjects, including 21 early and intermediate AMD subjects, and 24 age-matched controls. They observed that CC loss co-localized with drusen distribution and thus provided further evidence that drusen develop preferentially in areas of choroidal disruption.

In recent years, OCTA technology has provided an additional resource to study the pathogenesis of AMD. Several OCTA studies have investigated CC alterations in early and intermediate AMD eyes.[16,23] Our group recently investigated CC features in eyes affected by iAMD using SD-OCTA.[18] We retrospectively collected data from 42 eyes with iAMD (42 patients) and 20 healthy eyes (20 age-matched patients) who underwent SD-OCTA. In this study, we did not find differences in the total signal void area between bilateral iAMD and controls. However, the CC average flow void size was significantly greater in those iAMD eyes with neovascular AMD in the fellow eye. Fellow iAMD eyes of patients with unilateral neovascular AMD are known to be at a higher risk for the development of late AMD and therefore we speculated that our results support the theory that choroidopathy may be driving the development and progression of AMD.

However, the main limitation of these previous studies[16,18,23] relates to the use of SD-OCTA systems that may be more prone to shadowing artifacts from drusen. As a result, most of these studies were limited to evaluation of the CC in the drusen-free regions. The superiority of the SS-OCTA system in studying the CC under drusen was previously demonstrated by Lane and associates,[10] who designed a comparison study between SS-OCTA and SD-OCTA systems for evaluating flow impairment in early and intermediate AMD eyes. In this study, patients with drusen were imaged with both the SD-OCTA and SS-OCTA systems on the same day. Ambiguous OCTA CC dropout was defined as a low OCTA signal on the en face OCTA CC image with a corresponding low signal on the OCT en face scan. The authors concluded that the SS-OCTA system was significantly less prone to producing areas of false-positive flow impairment. The SS-OCTA system was also used to investigate the CC in eyes with nascent geographic atrophy (nGA) and/or drusen-associated geographic atrophy (DAGA).[24] In a study by Moult and associates,[24] a total of 7 eyes from 6 patients were imaged with OCTA, and several nGA and DAGA lesions were identified. The authors, based on their results, concluded that both nGA and DAGA regions were associated with focal CC flow impairment.

Therefore, the employment of SS-OCTA provided more reliable assessment of the CC in iAMD eyes and the capability to correlate several OCTA variables with the presence and extent of drusen.

To quantify the reduction of detected flow in the CC, we calculated the total signal void and the average flow void areas and we demonstrated that these variables were increased in iAMD eyes. Reduced CC flow may be the result of a reduced quantity of vessels (possibly the result of an increase in nonfunctional capillary segments known as ghost vessels[2] from histopathologic studies). Intermediate AMD eyes were also characterized by a reduced number of flow voids, which confirms the previously reported presence of an inverse relationship between flow void size and number.[16,25] We may speculate that intermediate AMD eyes are thus characterized by fewer CC vessels, which provide connection between contiguous intersinusoidal spaces. This convergence increases the flow voids' size and accordingly reduces their number.

One of the most notable observations from our study was that the reduction in CC perfusion is associated with drusen extent (area), rather than AMD status. Indeed, when analyzing iAMD status (diagnosis of iAMD or otherwise healthy eye) and cross-sectional area of drusen as covariates in the multiple regression analysis, we observed that drusen extent was a much stronger predictor of CC loss than AMD diagnosis. This analysis thus suggests a relationship between the choriocapillaris and drusen. The latter finding is further confirmed by the regional evaluation of the choriocapillaris. We demonstrated that the CC beneath drusen is characterized by an increased CC signal void area vs the drusen-free region.

In addition, we investigated the 150-μm-wide ring around the drusen border. Although these regions were not directly beneath drusen, we demonstrated increased CC loss in this neighboring area as well, indicating that CC abnormalities co-localized directly to the drusen as well as their bordering regions. The explanation of this finding may be intrinsic to the CC structure, which is known to be characterized by a propensity for capillary segments to be affected in the vicinity of an already nonfunctional segment.[2,16] Future studies investigating

the drusen-free region may provide additional substantive information regarding zonal differences in CC ischemia within this region and may identify whether CC perfusion progressively improves with greater distance from the drusen edge.

The mechanism(s) driving sub-RPE deposit formation, and the basis for the predilection of these deposits to form in areas associated with CC impairment, are unknown. Since the CC relies on VEGF secretion by the RPE, the presence of drusen could impair this trophic signaling process and lead to endothelial cell loss.[26] Alternatively, primary CC vascular loss, owing to inflammatory or degenerative mechanisms or other genetic and nongenetic factors, may lead to outer retinal layer dysfunction, with impaired washout of debris from the Bruch membrane and RPE ischemia.[27–29]

Our study has limitations, including the cross-sectional nature of the study. A prospective longitudinal evaluation of CC vascular density in intermediate AMD patients may shed further light on the causal role of the CC in drusen development. For example, it would be interesting to know whether drusen expand into neighboring areas of CC flow loss. Although we used a longer wavelength to image the CC, shadowing artifacts can still confound the analysis of the CC directly beneath drusen. However, we did use a novel method to compensate for the signal attenuation in the CC.[19] This methodology is based on the assumption that the shadowing effect under drusen may be identified as a decreased signal with both structural and flow CC images. In a recent paper by Zhang and associates,[19] the compensation was thus achieved by analyzing the structural information from the same slab used to image the blood flow in the CC. Notably, this study provided some confidence in the effectiveness of this method, given that the shadowing effect under drusen was compensated while the signal in the normal region remained the same. In addition, we also observed flow loss at the margin of drusen, which further supports our general conclusions. However, the image processing that we adopted is novel and may have limitations. Importantly, the noise level under drusen may be increased and this may have created an erroneous overestimation of flow in these regions. However, OCTA imaging is still a technology in evolution, and the optimal processing approaches have yet to be established. A final limitation is intrinsic to current OCTA technology, which may not be able to distinguish the absence of flow from slow flow below a detectable threshold range.

In summary, in this SS-OCTA study of the CC, we observed that eyes with intermediate AMD have reduced CC flow mainly confined to the CC beneath and surrounding drusen. Our results provide imaging evidence to support the histopathologic observation that drusen co-localize to regions of CC impairment. Future studies with longitudinal follow-up may provide further insight into the interrelationship between drusen, the choriocapillaris, and the pathogenesis of AMD.

REFERENCES

1. Curcio CA, Messinger JD, Sloan KR, McGwin G, Medeiros NE, Spaide RF. Subretinal drusenoid deposits in non-neovascular age-related macular degeneration: morphology, prevalence, topography, and biogenesis model. *Retina* 2013;33(2):265–276.

2. Mullins RF, Johnson MN, Faidley EA, Skeie JM, Huang J. Choriocapillaris vascular dropout related to density of drusen in human eyes with early age-related macular degeneration. *Invest Ophthalmol Vis Sci* 2011;52(3):1606–1612.

3. Ramrattan RS, van der Schaft TL, Mooy CM, de Bruijn WC, Mulder PG, de Jong PT. Morphometric analysis of Bruch's membrane, the choriocapillaris, and the choroid in aging. *Invest Ophthalmol Vis Sci* 1994;35(6):2857–2864.

4. Zarbin MA, Rosenfeld PJ. Pathway-based therapies for age-related macular degeneration: an integrated survey of emerging treatment alternatives. *Retina* 2010;30(9):1350–1367.

5. Querques G, Rosenfeld PJPJ, Cavallero E, et al. Treatment of dry age-related macular degeneration. *Ophthalmic Res* 2014;52(3):107–115.

6. Borrelli E, Abdelfattah NS, Uji A, Nittala MG, Boyer DS, Sadda SR. Postreceptor neuronal loss in intermediate age-related macular degeneration. *Am J Ophthalmol* 2017;181:1–11.

7. Spaide RF, Fujimoto JG, Waheed NK. Image artifacts in optical coherence tomography angiography. *Retina* 2015;35(11):2163–2180.

8. Choi W, Moult EM, Waheed NK, et al. Ultrahigh-speed, swept-source optical coherence tomography angiography in nonexudative age-related macular degeneration with geographic atrophy. *Ophthalmology* 2015;122(12):2532–2544.

9. Spaide RF. Choriocapillaris signal voids in maternally inherited diabetes and deafness and in pseudoxanthoma elasticum. *Retina* 2017;37(11):2008–2014.

10. Lane M, Moult EM, Novais EA, et al. Visualizing the choriocapillaris under drusen: comparing 1050-nm swept-source versus 840-nm spectral-domain optical coherence tomography angiography. *Invest Ophthalmol Vis Sci* 2016;57(9):OCT585.

11. Friedman E, Smith TR, Kuwabara T. Senile choroidal vascular patterns and drusen. *Arch Ophthalmol* 1963;69:220–230.

12. Sarks SH, Arnold JJ, Killingsworth MC, Sarks JP. Early drusen formation in the normal and aging eye and their relation to age related maculopathy: a clinicopathological study. *Br J Ophthalmol* 1999;83(3):358–368.

13. Holladay JT. Proper method for calculating average visual acuity. *J Refract Surg* 1997;13(4):388–391.

14. Nesper PL, Soetikno BT, Fawzi AA. Choriocapillaris nonperfusion is associated with poor visual acuity in eyes with reticular pseudodrusen. *Am J Ophthalmol* 2017;174:42–55.

15. Iafe NA, Phasukkijwatana N, Chen X, Sarraf D. Retinal capillary density and foveal avascular zone area are age-dependent: quantitative analysis using optical coherence tomography angiography. *Invest Opthalmol Vis Sci* 2016;57(13):5780.

16. Spaide RF. Choriocapillaris flow features follow a power law distribution: implications for characterization and mechanisms of disease progression. *Am J Ophthalmol* 2016;170:58–67.

17. Uji A, Balasubramanian S, Lei J, Baghdasaryan E, Al-Sheikh M, Sadda SR. Impact of multiple en face image averaging on quantitative assessment from optical coherence tomography angiography images. *Ophthalmology* 2017;124(7):944–952.

18. Borrelli E, Uji A, Sarraf D, Sadda SR. Alterations in the choriocapillaris in intermediate age-related macular degeneration. *Invest Opthalmol Vis Sci* 2017;58(11):4792–4798.

19. Zhang Q, Zheng F, Motulsky EH, et al. A novel strategy for quantifying choriocapillaris flow voids using swept-source OCT angiography. *Invest Opthalmol Vis Sci* 2018;59:203–211.

20. Schneider CA, Rasband WS, Eliceiri KW. NIH Image to ImageJ: 25 years of image analysis. *Nat Methods* 2012;9(7):671–675.

21. Uji A, Balasubramanian S, Lei J, Baghdasaryan E, Al-Sheikh M, Sadda SR. Choriocapillaris imaging using multiple en face optical coherence tomography angiography image averaging. *JAMA Ophthalmol* 2017;135(11):1197–1204.

22. Borrelli E, Lonngi M, Balasubramanian S, et al. Macular microvascular networks in healthy pediatric subjects. *Retina* 2018; https://doi.org/10.1097/IAE.0000000000002123. 2018.02.22.

23. Cicinelli MV, Rabiolo A, Marchese A, et al. Choroid morphometric analysis in non-neovascular age-related macular degeneration by means of optical coherence tomography angiography. *Br J Ophthalmol* 2017;101(9):1193–1200.

24. Moult EM, Waheed NK, Novais EA, et al. Swept-source optical coherence tomography angiography reveals choriocapillaris alterations in eyes with nascent geographic atrophy and drusen-associated geographic atrophy. *Retina* 2016;36:S2–11.

25. Al-Sheikh M, Phasukkijwatana N, Dolz-Marco R, et al. Quantitative OCT angiography of the retinal microvasculature and the choriocapillaris in myopic eyes. *Invest Opthalmol Vis Sci* 2017;58(4):2063–2069.

26. Saint-Geniez M, Kurihara T, Sekiyama E, Maldonado AE, D'Amore PA. An essential role for RPE-derived soluble VEGF in the maintenance of the choriocapillaris. *Proc Natl Acad Sci U S A* 2009;106(44):18751–18756.

27. Cabrera AP, Bhaskaran A, Xu J, et al. Senescence increases choroidal endothelial stiffness and susceptibility to complement injury: implications for choriocapillaris loss in AMD. *Invest Opthalmol Vis Sci* 2016;57(14):5910.

28. Moore DJ, Hussain AA, Marshall J. Age-related variation in the hydraulic conductivity of Bruch's membrane. *Invest Opthalmol Vis Sci* 1995;36(7):1290–1297.

29. Pilgrim MG, Lengyel I, Lanzirotti A, et al. Subretinal pigment epithelial deposition of drusen components including hydroxyapatite in a primary cell culture model. *Invest Opthalmol Vis Sci* 2017;58(2):708.